JOURNAL OF CATALYSIS 100, 86–94 (1986)

Structural, Surface, and Catalytic Properties of Bismuth Molybdovanadates Containing Foreign Atoms[1]

I. X-Ray Characterization of Iron-Containing Bismuth Molybdovanadate Catalysts

PIERO PORTA,[2] MARIANO LO JACONO, MARIO VALIGI, GIULIANO MINELLI, ANNA ANICHINI, SERGIO DE ROSSI, AND DELIA GAZZOLI

Centro di Studio del Consiglio Nazionale delle Ricerche (CNR) su "Struttura e Attività Catalitica di Sistemi di Ossidi" (SACSO), c/o Dipartimento di Chimica, Università "La Sapienza," 00185 Roma, Italy

Iron and bismuth molybdovanadates of general formula $Bi_{1-x/3}\square_{x/3-y}Me_y(V_{1-x}Mo_{x-y}Fe_y)O_4$, where Me = Fe or Bi, $\square$ = cation vacancy, with $x = 0.15, 0.30, 0.45, 0.60$, and 0.75 and $0 \leq y \leq x/3$, have been prepared by coprecipitation and final firing at 873 K. The structural characterization has been performed mainly by precise lattice parameter measurements but also by magnetic susceptibility studies. The X-ray data show that all specimens are monophasic with the scheelite tetragonal structure. The correlation between the lattice parameter a and compositional parameters x and y shows the effect of the cation and vacancy substitution on the unit cell lattice, which is interpreted in terms of the different ionic radii of the interchanging metal ions.

INTRODUCTION

Bismuth molybdates, iron-containing bismuth molybdates, and bismuth molybdovanadates have already received much attention as catalysts for selective oxidation, ammoxidation, and oxidative dehydrogenation of olefins to the corresponding unsaturated aldehydes, nitriles, and diolefins (*1*).

The high catalytic activity of the above compounds has been linked with the simultaneous presence of bismuth and cation vacancies (*2*). In principle, all selective (ammo)oxidation catalysts must possess redox properties, which are dependent upon the chemistry and the structure of both the surface and the bulk. In particular, they must be capable not only of undergoing reduction themselves giving the oxygen necessary for the olefin oxidation process, but also of being easily reoxidized by gaseous oxygen, thereby filling the vacancies created with O^{2-} during the first step.

The presence of a redox couple, such as Fe^{3+}/Fe^{2+}, in a catalyst can facilitate the redox processes by promoting electron and oxygen transfer between the surface and the bulk. Cation vacancies can also improve lattice oxygen diffusion and catalytic activity (*3*).

Some of the above compounds are known to crystallize in the ($CaWO_4$) scheelite-type structure, or in structures strictly derived from scheelite (*2*).

In the ideal body-centered tetragonal (space group $I4_1/a$) ABO_4-type scheelite structure the B cation is usually hexavalent and tetrahedrally coordinated by oxygen, while the A cation is usually divalent and eight-coordinated by oxygens from eight different $(BO_4)^{2-}$ tetrahedra.

A wide variety of chemistry for compounds with the scheelite structure has so far been explored. A few possibilities for anions different from oxygen, namely fluorine and nitrogen, are known in scheelite chemistry, but many different A and B cat-

[1] This work has been supported by a financial contribution from the "Progetto Finalizzato (CNR) on Chimica Fine e Secondaria."

[2] To whom correspondence should be addressed.

0021-9517/86 $3.00

ions with various oxidation states may easily be accommodated in the scheelite lattice, the main restriction for the latter possibility being that the cations must be capable, respectively, of eight-fold and tetrahedral coordination to oxygen. Some examples which illustrate the variety of possible cation oxidation states in oxides with the scheelite structure are $KReO_4$, $CaWO_4$ (mineral scheelite), $BiVO_4$ (high-temperature form, above 600 K), and $ZrGeO_4$ (*2*).

The α-phase of bismuth molybdate, $Bi_2(MoO_4)_3$, has been shown from both powder (*4*) and single-crystal (*5*) X-ray diffraction studies to crystallize with a monoclinic superstructure derived from the $CaWO_4$–scheelite structure, where three of the A cations are replaced by two trivalent cations, such as Bi^{3+}, producing a cation vacancy in the lattice, and so giving a chemical formula which is more correctly written as $Bi_2\square(MoO_4)_3$, where $\square$ represents a vacant eight-coordinated cation site.

Some ternary compounds containing atoms other than bismuth and molybdenum are known to be derived from the α-phase of bismuth molybdate. For example, the Bi–V–Mo-based oxidic compounds have been proved to crystallize in the tetragonal scheelite-type structure which persists over almost the entire range of $Bi_{1-x/3}\square_{x/3}(V_{1-x}Mo_x)O_4$ solid solution formation (in particular, from $x = 0.1$ to values close to unity, where the monoclinic α-phase of bismuth molybdate is present), and where a controlled number of vacancies occurs in order to preserve charge neutrality (*4*). This class of compounds has been successfully used as catalysts for the (ammo)oxidation of olefins (*6*). Among the ternary Bi–Fe–Mo-based oxides two compounds of formula $Bi_3(FeMo_2)O_{12}$ (*7*, *8*) and $Bi_2Fe(FeMo_2)O_{12}$ (*8*) have also been reported to exist, and found to exhibit high catalytic activity and selectivity toward olefin oxidation (*9–12*). Their structure is strictly derived from the scheelite-type α-bismuth molybdate, $Bi_2\square(MoO_4)_3$, by simultaneously replacing one tetrahedral Mo^{6+} ion and one eight-coordinated vacant site with one Fe^{3+} and one Bi^{3+} ion ($Mo^{6+} + \square \leftrightarrow Fe^{3+} + Bi^{3+}$), or with two Fe^{3+} ions ($Mo^{6+} + \square \leftrightarrow 2Fe^{3+}$), respectively.

Taking into account all the above mentioned studies we thought it would be interesting to initiate an investigation on iron-containing bismuth molybdovanadates of general formula

$$Bi_{1-x/3}\square_{x/3-y}Me_y(V_{1-x}Mo_{x-y}Fe_y)O_4,$$

where *Me* = Fe or Bi and $\square$ = cation vacancy, with the aim of: (i) obtaining new multicomponent oxide catalysts which preserve the scheelite structure over a wide range of x and y compositions and have controlled amounts of cation vacancies, (ii) determining their structural properties, both bulk and surface, and (iii) finding a correlation between structural properties and their catalytic behavior toward some oxidation and dehydrogenation reactions.

This paper refers mainly to the X-ray characterization of the catalysts. Forthcoming papers will deal with a detailed study embracing EPR and further magnetic work, together with investigations of the reducibility and surface properties, the catalyzed oxidation of propene to acrolein, and the catalyzed dehydrogenation of 1-butene to butadiene.

EXPERIMENTAL

Preparation and analysis. All the chemicals used in the preparation of the samples were of analytical grade. The compounds were prepared by coprecipitation from a solution of $(NH_4)_6Mo_7O_{24}$ and an ammonia suspension of NH_4VO_3 with $Bi(NO_3)_3$ in acidic solution by HNO_3 (*13*). In the case of iron-containing samples an iron nitrate solution was also added. The quantities of the different solutions were varied in order to achieve compositions with $x = 0.15$, 0.30, 0.45, 0.60, and 0.75, and y varying, for each value of x, from zero to $x/3$ in steps of 0.05. The suspension was stirred at 353 K until

TABLE 1

List of the Studied $Bi_{1-x/3}\square_{x/3-y}Me_y(V_{1-x}Mo_{x-y}Fe_y)O_4$ Samples with Their Metal Chemical Composition; for Each Sample the Weight Percent, Both Nominal and Experimental, Are Given

Sample		$\%Bi_{nom.}$	$\%Bi_{exp.}$	$\%Fe_{nom.}$	$\%Fe_{exp.}$	$\%Mo_{nom.}$	$\%Mo_{exp.}$	$\%V_{nom.}$	$\%V_{exp.}$
For *Me* = Fe:									
x	2*y*								
0.15	0.00	62.0	62.3	—	—	4.49	5.29	13.52	13.88
0.15	0.10	61.8	58.0	1.74	1.75	3.38	3.56	13.49	13.53
0.30	0.00	59.4	61.5	—	—	9.09	9.26	11.26	11.72
0.30	0.10	59.3	56.8	1.76	1.82	7.56	8.28	11.24	10.98
0.30	0.20	59.1	55.5	3.52	3.55	6.03	6.67	11.21	11.58
0.45	0.00	56.8	58.0	—	—	13.80	14.49	8.95	8.80
0.45	0.10	56.6	52.4	1.78	1.84	12.37	13.36	8.93	8.84
0.45	0.20	56.5	53.0	3.55	3.55	10.34	11.59	8.91	8.82
0.45	0.30	56.3	52.7	5.31	5.16	8.79	9.88	8.89	8.83
0.60	0.00	54.0	50.0	—	—	18.62	19.26	6.59	6.91
0.60	0.10	53.9	49.8	1.80	1.86	17.00	18.17	6.57	6.97
0.60	0.20	53.8	50.0	3.59	3.59	15.46	15.72	6.55	6.97
0.60	0.30	53.7	49.8	5.38	5.21	13.87	14.41	6.54	7.10
0.60	0.40	53.5	49.7	7.15	6.90	12.29	12.49	6.52	7.36
0.75	0.00	51.3	49.0	—	—	23.55	24.67	4.17	4.17
0.75	0.10	51.2	49.0	1.82	1.89	21.91	22.54	4.16	3.95
0.75	0.20	51.0	49.1	3.64	3.67	20.30	20.34	4.15	4.49
0.75	0.30	51.0	48.8	5.44	5.24	18.72	18.65	4.12	4.61
0.75	0.40	50.8	47.2	7.24	7.05	17.10	17.18	4.13	4.90
0.75	0.50	50.6	48.4	9.03	8.70	15.50	15.08	4.12	4.61
For *Me* = Bi									
x	2*y*								
0.45	0.10	58.5	54.5	0.87	0.91	11.88	12.88	8.72	7.73
0.45	0.20	60.2	56.0	1.69	1.74	10.18	11.02	8.50	8.22
0.45	0.30	61.8	56.6	2.48	2.49	8.55	9.25	8.28	7.97
0.60	0.10	55.9	52.6	0.88	0.92	16.61	18.03	6.41	6.17
0.60	0.20	57.7	54.5	1.71	1.75	14.71	15.07	6.25	6.45
0.60	0.30	59.3	54.9	2.47	2.63	12.91	13.92	6.09	6.17
0.60	0.40	60.9	55.8	3.26	3.39	11.19	10.54	5.94	5.94

the evaporation was almost complete. The product was then dried at 383 K, ground and heated to 573 K in order to decompose the nitrates. The specimens were then reground, and finally heated in air at 873 K for 24 h.

The color of the samples ranged from pale yellow to orange–light brown depending on the different compositions, and especially the iron content.

The content of all metals was determined by atomic absorption using a Varian AA5 instrument, and was found to be in good agreement with the nominal concentration. Table 1 reports the results of the chemical analysis.

X-Ray analysis. The powder diffraction patterns were first recorded with a Geiger counter Philips spectrogoniometer and Cu$K\alpha$ (Ni-filtered) radiation for the phase analysis. For the determination of the lattice parameters a Debye–Scherrer camera (internal diameter of 114.6 mm, with Straumanis film mounting) and Cr$K\alpha$ (V-filtered) radiation were used. This radiation was chosen since it gives well-resolved X-ray reflections in the back-reflection region and, most important, since it allows one to detect the (420) reflection, independent of the c parameter and at $\theta \simeq 80°$, thereby leading to a very high precision on the measurement of the lattice parameter a.

The following seven reflections, in the back-reflection region of $\theta = 60$ to 90°, were recorded (the first figure showing the Miller index and the second, in parentheses, the approximate mean value of the θ Bragg angle for each reflection): 400 (62°), 208 (64°),

316 (66°), 325 (68°), 413 (73°), 404 (75°), 420 (80°).

The spectra of samples without iron showed a minor resolution of α_1–α_2 doublets as compared with the iron-containing specimens, thus indicating a higher crystallinity in the latter compounds.

The positions of the reflections were read visually by means of a Philips measuring device with an accuracy of ±0.005 cm and were then used in constructing Nelson–Riley plots for extrapolation to $\theta = 90°$, thereby evaluating the unit cell parameter a. The axial ratio $C = a/c$ was determined by minimizing the deviations of the a values following a least-squares procedure. For samples without iron, where the uncertainty is higher because of the poorly resolved α_1–α_2 doublets, the error in a, c, and V is ±0.001 Å, ±0.02 Å, and 0.5 Å^3, respectively, whereas for iron-containing specimens the error is ±0.0005 Å, ±0.01 Å, and ±0.1 Å^3, respectively.

Magnetic susceptibility. Magnetic susceptibility measurements were performed by the Gouy method at different field strengths (4000, 6000, and 8000 g) and in the temperature range 78 to 300 K. A semimi-

TABLE 2

List of the Studied $Bi_{1-x/3}\square_{x/3-y}Me_y(V_{1-x}Mo_{x-y}Fe_y)O_4$ Samples with Their Metal Chemical Composition (Molar Fraction), Lattice Parameters a (Å) and c (Å), and Cell Volume V (Å^3)

Sample		In eight-coordinated sites			In tetrahedral sites					
For *Me* = Fe		Bi	□	Fe	V	Mo	Fe	a	c	V
x	$2y$									
0.15	0.00	0.95	0.05	—	0.85	0.15	—	5.161	11.69	311.4
0.15	0.10	0.95	—	0.05	0.85	0.10	0.05	5.166	11.68	311.7
0.30	0.00	0.90	0.10	—	0.70	0.30	—	5.182	11.68	313.6
0.30	0.10	0.90	0.05	0.05	0.70	0.25	0.05	5.179	11.69	313.5
0.30	0.20	0.90	—	0.10	0.70	0.20	0.10	5.186	11.69	314.4
0.45	0.00	0.85	0.15	—	0.55	0.45	—	5.199	11.70	316.2
0.45	0.10	0.85	0.10	0.05	0.55	0.40	0.05	5.201	11.69	316.2
0.45	0.20	0.85	0.05	0.10	0.55	0.35	0.10	5.198	11.69	315.8
0.45	0.30	0.85	—	0.15	0.55	0.30	0.15	5.204	11.70	316.8
0.60	0.00	0.80	0.20	—	0.40	0.60	—	5.226	11.68	319.0
0.60	0.10	0.80	0.15	0.05	0.40	0.55	0.05	5.227	11.70	319.7
0.60	0.20	0.80	0.10	0.10	0.40	0.50	0.10	5.226	11.70	319.5
0.60	0.30	0.80	0.05	0.15	0.40	0.45	0.15	5.227	11.69	319.4
0.60	0.40	0.80	—	0.20	0.40	0.40	0.20	5.230	11.67	319.2
0.75	0.00	0.75	0.25	—	0.25	0.75	—	5.241	11.69	321.3
0.75	0.10	0.75	0.20	0.05	0.25	0.70	0.05	5.246	11.73	322.8
0.75	0.20	0.75	0.15	0.10	0.25	0.65	0.10	5.253	11.69	322.6
0.75	0.30	0.75	0.10	0.15	0.25	0.60	0.15	5.253	11.68	322.3
0.75	0.40	0.75	0.05	0.20	0.25	0.55	0.20	5.254	11.67	322.1
0.75	0.50	0.75	—	0.25	0.25	0.50	0.25	5.256	11.74	324.3
For *Me* = Bi										
x	$2y$									
0.45	0.10	0.90	0.10	—	0.55	0.40	0.05	5.215	11.69	317.9
0.45	0.20	0.95	0.05	—	0.55	0.35	0.10	5.225	11.68	318.9
0.45	0.30	1.00	—	—	0.55	0.30	0.15	5.221	11.65	317.6
0.60	0.10	0.85	0.15	—	0.40	0.55	0.05	5.228	11.70	319.7
0.60	0.20	0.90	0.10	—	0.40	0.50	0.10	5.235	11.69	320.4
0.60	0.30	0.95	0.05	—	0.40	0.45	0.15	5.243	11.68	321.0
0.60	0.40	1.00	—	—	0.40	0.40	0.20	5.247	11.68	321.6

crobalance reading to ±0.01 mg was employed. The apparatus was calibrated with $Hg[Co(CNS)_4]$. The samples were found to be field independent and to obey the Curie–Weiss law $\chi_{at.} = C/(T - \theta)$ in the whole temperature range.

RESULTS

Table 2 reports the list of the prepared samples together with their detailed nominal chemical composition in molar fraction, and their unit cell parameters.

First, it should be pointed out that the X-ray patterns of all compounds are very similar to the pattern of the bismuth molybdovanadates (*6*) and to that of the mineral scheelite, $CaWO_4$ (*14*). Table 3 reports the interplanar spacings d and the visually estimated intensities for one of the prepared samples (all compounds show the same X-ray pattern), together with the data reported in the literature for $CaWO_4$ (*14*). No lines other than those belonging to the tetragonal scheelite structure (space group $I4_1/a$) (*15*) appear on the X-ray films taken with different radiations and after very long exposure.

It may be seen from Table 2 that the unit cell parameter c is not remarkably affected by composition, whereas for the a parameter a complex influence is observed when changing x and/or $2y$. Figures 1, 2, and 3 show the correlations between the lattice parameter a and the compositional parameters x and $2y$, which will be discussed in detail for the three series of compounds in the next section.

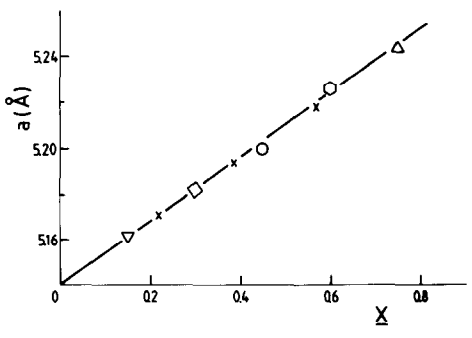

FIG. 1. Lattice parameter a vs x composition in $Bi_{1-x/3}\square_{x/3}(V_{1-x}Mo_x)O_4$ solid solutions ($\square$ = cation vacancies). (∇) $x = 0.15$; ($\diamond$) $x = 0.30$; ($\bigcirc$) $x = 0.45$; ($\bigcirc$) $x = 0.60$; ($\triangle$) $x = 0.75$. The error limits in a are smaller than the diameter of the polygons used to indicate the experimental points. The results from Cesari *et. al.* (Ref. (*4*)) are also reported (cross points).

TABLE 3

Interplanar Spacings, d (Å), and Intensities, I, Taken from the X-Ray Spectrum of One of the $Bi_{1-x/3}\square_{x/3-y}Me_y(V_{1-x}Mo_{x-y}Fe_y)O_4$ Samples, Namely that where Me = Fe and $x = 0.60$, $2y = 0.40$

Our sample[a]		$CaWO_4$		
d	I[b]	d	I/I_1	hkl
4.76	m	4.77	70	101
3.11	vs	3.11	100	103
2.91	m	2.85	50	004
2.61	m	2.63	60	200
2.29	m	2.30	60	211
2.13	w	2.09	40	105
2.00	w	2.00	50	213
1.95	s	1.94	80	204
1.85	w	1.857	60	220
1.72	s	1.691	70	116
1.64	vw	1.636	50	215
1.58	s	1.596	90	303
1.56	w	1.558	70	224
1.46	vvw	1.425	20	008
1.43	vvw	1.446	50	321
1.35	vvw	1.338	50	217
1.30	vvw	1.313	50	400
1.27	w	1.251	80	208–316
1.255	m			
1.225	vw	1.230	20	325
1.198	w	1.210	60	413
1.186	w	1.193	60	404
1.164	w	1.178	50	420

Note. Interplanar spacings, d, intensities, I, and Miller indexes, hkl, for the mineral "scheelite," $CaWO_4$ (Ref. (*14*)), are also reported for comparison.

[a] The X-ray patterns of all other samples are very similar to those reported in this table.

[b] Visually estimated intensities: vs = very strong, s = strong, m = medium, w = weak, vw = very weak, vvw = very very weak.

Regarding the magnetic results, the specimens without iron were found to be diamagnetic, whereas values of the magnetic moment μ around 5.95 B.M. were observed for all the compounds containing iron. No ferromagnetic behavior was no-

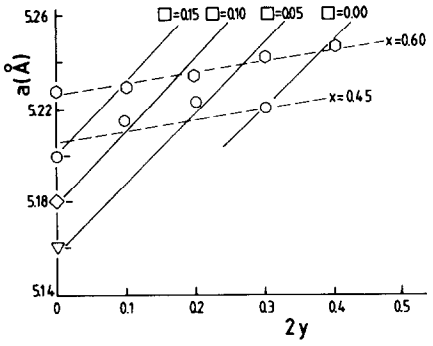

FIG. 2. Lattice parameter a vs $2y$ (Bi + Fe) composition in $Bi_{1-x/3+y}\square_{x/3-y}(V_{1-x}Mo_{x-y}Fe_y)O_4$ solid solutions (□ = cation vacancies). (▽) $x = 0.15$; (◇) $x = 0.30$; (○) $x = 0.45$; (○) $x = 0.60$. The error limits in a are smaller than the diameter of the polygons used to indicate the experimental points.

ticed in the iron-containing specimens. The values of the Weiss temperature θ, taken from the intercepts on the plots of $1/\chi_{at.}$ vs T, were found to increase with increasing iron content within each series of samples.

DISCUSSION

The presence of only one scheelite phase and the variation of the lattice parameter a, which is more sensitive to cation substitution than the c parameter of the tetragonal lattice, establish the formation of a solid solution for samples both with and without iron. In the first case the iron incorporation takes place as Fe^{3+}, as indicated by the magnetic measurements. The observed value for the magnetic moment is around 5.95 B.M. as expected for Fe^{3+} in the $3d^5$ high-spin configuration.

In order to confirm the occurrence of a complete solid solution and to ascertain the absence of other phases containing iron, such as α-Fe_2O_3, in quantity not easily detectable by X-ray, a mechanical mixture was made between a bismuth molybdovanadate, namely that of formula $Bi_{0.8}\square_{0.2}(V_{0.4}Mo_{0.6})O_4$, and α-Fe_2O_3 in such quantities that the iron content was comparable to that present in the sample of formula $Bi_{0.8}Fe_{0.2}(V_{0.4}Mo_{0.4}Fe_{0.2})O_4$. The magnetic susceptibility of the mechanical mixture has been found to slightly increase with increasing temperature ($\chi_{at.}$ at 150 K = 1×10^{-3}, $\chi_{at.}$ at 295 K = 2.4×10^{-3} cgs units) so confirming the typical magnetic behaviour of α-Fe_2O_3 (*16*). On the contrary, our sample, $Bi_{0.8}Fe_{0.2}(V_{0.4}Mo_{0.4}Fe_{0.2})O_4$, as any of the other studied compounds, follows the Curie–Weiss law, that is the magnetic susceptibility decreases with increasing temperature ($\chi_{at.}$ at 150 K = 1.4×10^{-2}, $\chi_{at.}$ at 295 K = 1×10^{-2} cgs units), as expected for Fe^{3+}-containing compounds (*16*).

The correlation between lattice parameter variation and cation substitution will now be examined. For the sake of clarity the discussion will be divided into three sections. The first one will consider the samples without iron, the second part will deal with those specimens containing iron only in the tetrahedral sites of the scheelite structure, and the third series, comprising the majority of the samples, will discuss the most interesting solid solutions, i.e., those containing iron in both tetrahedral and eight-coordinated lattice sites.

For a better illustration of the correlation between observed and expected lattice variations in the iron-containing samples, i.e., both series 2 and 3, all the substitutional mechanisms involved in the solid solution formation are schematically reported

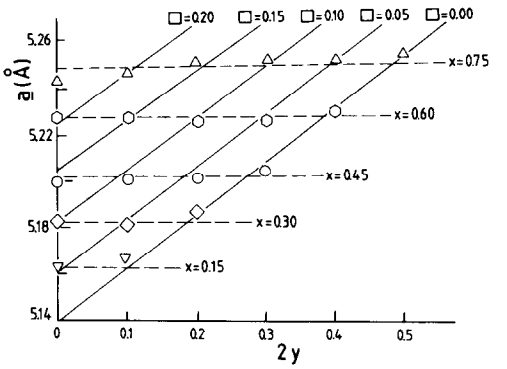

FIG. 3. Lattice parameter a vs $2y$ (Fe) composition in $Bi_{1-x/3}\square_{x/3-y}Fe_y(V_{1-x}Mo_{x-y}Fe_y)O_4$ solid solutions (□ = cation vacancies). (▽) $x = 0.15$; (◇) $x = 0.30$; (○) $x = 0.45$; (○) 0.60; (△) $x = 0.75$. The error limits in a are smaller than the diameter of the polygons used to indicate the experimental points.

in Table 4, where Shannon's ionic radii (*17*) are also given. Moreover, the series 2 and 3 will be discussed separately (see also Table 4) for given and constant values of: (i) cation vacancy, (ii) compositional parameter $2y$, and (iii) compositional parameter x.

1. $Bi_{1-x/3}\square_{x/3}(V_{1-x}Mo_{x-y})O_4$ series. These solid solutions originate from Bi VO_4 where x Mo^{6+} replaces an equivalent amount of V^{5+} ions in the tetrahedral sites and leaves $x/3$ eight-coordinated cation vacancies; this system has already been studied by Cesari *et al.* (*4*) at $x = 0.21$, 0.37, and 0.55, and their results, reported in Fig. 1 as crosses, are in good agreement with our findings. All samples show an increase of a with increase of x, i.e., of molybdenum content. This behavior is easily explained by the substitutional mechanism which justifies the lattice expansion. In fact, by incorporation of Mo^{6+} ions in $BiVO_4$, a double expansion effect on the lattice must be expected: one is due to x Mo^{6+} replacing x V^{5+} in the tetrahedral sites (the tetrahedral ionic radii for Mo^{6+} and V^{5+} are, according to Shannon (*17*), 0.41 and 0.355 Å, respectively), and another predictable expansion (*18, 19*) is due to a simultaneous creation of $x/3$ cation vacancies in the eight-coordinated sublattice.

2. $Bi_{1-x/3+y}\square_{x/3-y}(V_{1-x}Mo_{x-y}Fe_y)O_4$ series. These compounds can be thought as derived from the bismuth molybdovanadates, series 1, where y Fe^{3+} + y Bi^{3+} replace y Mo^{6+}, the Fe^{3+} ions interchanging with Mo^{6+} in the tetrahedral sites, and the Bi^{3+} ions filling an equivalent amount of eight-coordinated cation vacancies in order to preserve charge neutrality.

The variation of the unit cell parameter a with the compositional parameter $2y$ is shown for this series in Fig. 2.

(i) It may first be noted from Fig. 2 that for equal values of cation vacancies the lattice parameter strongly increases with increasing of both x and $2y$ (full lines in the figure). Since the substitutional mechanism correlated with increase of x and $2y$ is $Mo^{6+} \rightarrow V^{5+}$ and $Fe^{3+} \rightarrow V^{5+}$ in the tetrahedral sites, the sharp increase in a is in agreement with expectations (difference in ionic radii, Table 4).

(ii) The second observation on this series is that for equal values of $2y$, that is y bismuth + y iron, but both x and vacancies increasing, an increase of the lattice parameter a is found (points lying on lines perpendicular to the axis of abscissae in Fig. 2). For these compositional changes and according to the scheme shown in Ta-

TABLE 4

Mechanisms of Cation Substitutions in the $Bi_{1-x/3}\square_{x/3-y}Me_y(V_{1-x}Mo_{x-y}Fe_y)O_4$ Solid Solution Formation, Expected Lattice Parameter Variations on the Basis of Ionic Radii Considerations,[a] and Experimentally Observed Lattice Parameter Variations

	For *Me* = Bi			For *Me* = Fe		
	Substitutions	$\Delta a_{expected}$	$\Delta a_{observed}$	Substitutions	$\Delta a_{expected}$	$\Delta a_{observed}$
(i) For equal values of □ (x and $2y$ increase)	Mo → V Fe → V	Positive Positive	Positive (very strong)	Mo → V Fe → V Fe → Bi	Positive Positive Negative	Positive (strong)
(ii) For equal values of $2y$ (x and □ increase)	Mo → V □ → Bi	Positive Positive	Positive (strong)	Mo → V □ → Bi	Positive Positive	Positive (strong)
(iii) For equal values of x (y and □ variable)	Fe → Mo Bi → □	Positive Negative	Positive (weak)	Fe → Mo Fe → □	Positive Negative	No effect

[a] Shannon's ionic radii (Ref. (*17*)). Tetrahedral: Fe^{3+} (high-spin) = 0.49; Mo^{6+} = 0.41; V^{5+} = 0.355 Å. Eight-coordinated: Bi^{3+} = 1.17; Fe^{3+} (estimated) = 0.78 Å.

ble 4, the substitutions which take place here, i.e., $Mo^{6+} \rightarrow V^{5+}$ and $\square \rightarrow Bi^{3+}$, both tend, as observed, to expand the lattice.

(iii) It may finally be noted for this series that a slight increase of a is observed for equal values of x (constant vanadium content), as shown from the dashed lines in Fig. 2. The observed increase of a may be interpreted by the following concomitant substitutional processes: $Fe^{3+} \rightarrow Mo^{6+}$ in the tetrahedral sites, which would cause a lattice expansion (see Shannon's radii in Table 4), and $Bi^{3+} \rightarrow \square$ in the eight-coordinated sites which would presumably give a theoretically expected lattice contraction (*18, 19*). These two opposite effects nearly compensate.

3. $Bi_{1-x/3}\square_{x/3-y}Fe_y(V_{1-x}Mo_{x-y}Fe_y)O_4$ series. The replacement of y Mo^{6+} in the bismuth molybdovanadates (series 1) by $2y$ Fe^{3+} ions give rise to the third series of solid solutions, with iron substituting molybdenum in the tetrahedral sites and simultaneously filling an equivalent amount of eight-coordinated cation vacancies.

The variation of the lattice parameter a with the compositional parameter $2y$ is shown in Fig. 3.

(i) The increase of the lattice parameter with increasing of both x and $2y$, and for equal values of cation vacancy content, is disclosed by the full lines. In this case, as depicted in Table 4, the increase of a is due to two lattice expansion effects in the tetrahedral sublattice according to the following replacements: $Mo^{6+} \rightarrow V^{5+}$ and $Fe^{3+} \rightarrow V^{5+}$, and to a lattice contraction due to Fe^{3+} substituting Bi^{3+} in the eight-coordinated sites, which as a whole leads to an overall expansion of the lattice. The observed positive variation of a is, as expected, less evident in this case than in the second series where only the two equivalent expansion effects are present.

(ii) An increase of a is, moreover, observed for samples having equal values of $2y$ (iron) and both x and vacancy contents increasing (points lying on lines perpendicular to the axis of the abscissae in Fig.3). The behavior here, as in the similar situation of the second series, is interpreted in terms of the double lattice expansion effect caused by the substitutional mechanisms (see Table 4): $Mo^{6+} \rightarrow V^{5+}$ in the tetrahedral sublattice, and $\square \rightarrow Bi^{3+}$ in the eight-coordinated one.

(iii) A near constancy of a values is finally found for samples at equal values of x, and both $2y$ and vacancies variable (dashed lines in Fig. 3). As shown in Table 4 the interchanging mechanisms are in this case as follows: $Fe^{3+} \rightarrow Mo^{6+}$ in the tetrahedral sites, which would cause an expansion of the lattice, and $Fe^{3+} \rightarrow \square$ in the eight-coordinated sites with expected lattice contraction. These two opposite effects seem to nearly compensate. The near constancy of a observed in this case as compared with the slightly positive Δa variation noticed in the second series of samples (similar cases for equal values of x in Table 4) may be explained by the fact that the filling of vacancies by Fe^{3+} (estimated eight-coordinated ionic radius equal to 0.78 Å (*17*)) produces a higher lattice contraction than that caused in the second series (eight-coordinated Bi^{3+} ionic radius equal to 1.17 Å).

In addition to the clear evidence drawn from the lattice parameter variation, the presence in the second series of only one type of iron, namely the tetrahedrally coordinated one, and in third series of both tetrahedral and eight-coordinated Fe^{3+}, has been revealed from both EPR and magnetic susceptibility measurements, and this will be the subject of a forthcoming communication.

As far as the site symmetry of Fe^{3+} ions is concerned, it may be recalled that several investigations on the $Bi_3(FeMo_2)O_{12}$ compound (*7–11*) have well established the presence of iron in the tetrahedral sublattice of molybdenum, whereas some disagreement exists for the presence of Fe^{3+} ions in the eight-coordinated sublattice of bismuth (*7–9*). In particular, while some authors tend to exclude (*7, 9*) the possible existence of eight-coordinated iron, others (*8,*

10, 11) claimed for the occurrence of eight-coordinated Fe^{3+} if favorable crystallographic circumstances, such as in the $Bi_2Fe(FeMo_2)O_{12}$ compound, are present. Moreover, a recent investigation performed by Grzybowska *et al.* (*20*) by means of Raman, IR, and XPS methods on the Bi–Fe–Mo–O system has confirmed the existence of the $Bi_2Fe(FeMo_2)O_{12}$ compound previously studied by Lo Jacono *et al.* (*8*), other than the $Bi_3(FeMo_2)O_{12}$ compound which, according to other authors (*7, 9*), seemed to be the only definite compound in this system.

We are well aware of the difficulty for such small ions as Fe^{3+} to achieve eight-coordination to oxygen (no compounds with Fe^{3+} in this site symmetry have been proved by single-crystal X-ray diffraction to exist); however, in the system studied by us (the third series of samples) there are indeed eight-coordinated cation vacancies into the lattice which could be filled by iron and the results all point to corroborate this behavior. It should also be recalled that the X-ray spectra have revealed a higher crystallinity for the samples of the third series, that is, those containing iron in both lattice sites. This observation suggests that the filling up of eight-coordinated cation vacancies by iron, in spite of its small size, leads to a better crystal lattice stabilization.

ACKNOWLEDGMENTS

The authors would like to thank Professor A. Cimino for critically reading the manuscript and Mr. M. Inversi for the drawings.

REFERENCES

1. Keulks, G. W., Krenzke, L. D., and Notermann, T. N., "Advances in Catalysis," Vol. 27, p. 183. Academic Press, New York, 1978; Bielanski, A., and Haber, J., *Catal. Rev. Sci. Eng.* **19,** 1 (1979); Brazdil, J. F., Suresh, D. D., and Grasselli, R. K., *J. Catal.* **66,** 347 (1980); Grasselli, R. K., and Burrington, J. D., "Advances in Catalysis," Vol. 30, p. 133. Academic Press, New York, 1981; and other references in all those papers.
2. Sleight, A. W., *in* "Advanced Materials in Catalysis" (J. J. Burton and R. L. Ganten, Eds.), pp. 181–208. Academic Press, New York, 1977.
3. Brazdil, J. F., Glaeser, L. C., and Grasselli, R. K., *J. Catal.* **81,** 142 (1983).
4. Cesari, M., Perego, G., Zazzetta, A., Manara, G., and Notari, B., *J. Inorg. Nucl. Chem.* **33,** 3595 (1971).
5. van den Elzen, A. F., and Rieck, G. D., *Acta Crystallogr. Sect. B* **29,** 2433 (1973).
6. Notari, B., Cesari, M., Manara, G., and Perego, G., U.S. Patent 3,492,248 (1976).
7. Jeitschko, W., Sleight, A. W., McClellan, W. R., and Weiher, J. F., *Acta Crystallogr. Sect. B* **32,** 1163 (1976).
8. Lo Jacono, M., Notermann, T., and Keulks, G. W., *J. Catal.* **40,** 19 (1975).
9. Linn, W. J., and Sleight, A. W., *J. Catal.* **41,** 134 (1976).
10. Krenzke, L. D., and Keulks, G. W., *J. Catal.* **64,** 295 (1980).
11. Notermann, T., Keulks, G. W., Shkarov, A., Maximov, Y. U., Margolis, L. Ya., and Krylov, O. V., *J. Catal.* **39,** 286 (1975).
12. Bruckman, K., and Grzybowska, B., *React. Kinet. Catal. Lett.* **26,** 117 (1984).
13. Anichini, A., De Rossi, S., Gazzoli, D., Lo Jacono, M., Minelli, G., Porta, P., and Valigi, M., Ital. Patent 49573A81 (1981).
14. Powder Diffraction File, Inorganic Volume, Chart N° 8-145, p. 317. Amer. Soc. Testing Materials, Philadelphia, 1967.
15. "International Tables for X-Ray Crystallography," Vol. I, p. 178. Kynoch Press, Birmingham, England, 1952.
16. Schieber, M. M., "Experimental Magnetochemistry," Vol. VIII, p. 168. North-Holland, Amsterdam (1967).
17. Shannon, R. D., *Acta Crystallogr. Sect. A* **32,** 751 (1976).
18. Mott., N. F., and Littleton, M. J., *Trans. Faraday. Soc.* **34,** 485 (1938).
19. Cimino, A., and Marezio, M., *J. Phys. Chem. Solids* **17,** 57 (1960).
20. Grzybowska, B., Payen, E., Gengembre, L., and Bonnelle, J. P., *Bull. Pol. Acad. Sci.* **31,** 245 (1983).